

# Bioactive Aliphatic Polycarbonates Carrying Guanidinium Functions: An Innovative Approach for Myotonic Dystrophy Type 1 Therapy

Alexandra Baroni,<sup>†,‡</sup> Ioan Neaga,<sup>†,§</sup> Nicolas Delbos,<sup>‡</sup> Mathilde Wells,<sup>†</sup> Laetitia Verdy,<sup>†</sup> Eugénie Anseau,<sup>||</sup> Jean Jacques Vanden Eynde,<sup>⊥</sup> Alexandra Belayew,<sup>||</sup> Ede Bodoki,<sup>§,ib</sup> Radu Oprean,<sup>§</sup> Stéphanie Hambye,<sup>\*,†</sup> and Bertrand Blankert<sup>\*,†,ib</sup>

<sup>†</sup>Laboratory of Pharmaceutical Analysis, Faculty of Medicine and Pharmacy, Research Institute for Health Sciences and Technology,

<sup>||</sup>Laboratory of Molecular Biology, Faculty of Medicine and Pharmacy, Research Institute for Health Sciences and Technology, and

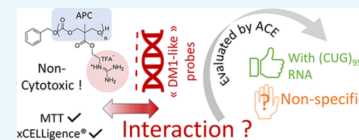
<sup>⊥</sup>Laboratory of Organic Chemistry, Faculty of Sciences, University of Mons, Place du Parc 20, 7000 Mons, Belgium

<sup>‡</sup>Laboratory of Polymeric and Composite Materials, Center of Innovation and Research in Materials and Polymers (CIRMAP), University of Mons. 20 Place du Parc, 7000 Mons, Belgium

<sup>§</sup>Analytical Chemistry Department, “Iuliu Hațieganu” University of Medicine and Pharmacy, 4, Louis Pasteur Street, 400349 Cluj-Napoca, Romania

## Supporting Information

**ABSTRACT:** *Dystrophia myotonica* type 1 (DM1) results from nuclear sequestration of splicing factors by a messenger RNA (mRNA) harboring a large (CUG)<sub>n</sub> repeat array transcribed from the causal (CTG)<sub>n</sub> DNA amplification. Several compounds were previously shown to bind the (CUG)<sub>n</sub> RNA and release the splicing factors. We now investigated for the first time the interaction of an aliphatic polycarbonate carrying guanidinium functions to DM1 DNA/RNA model probes by affinity capillary electrophoresis. The apparent association constants ( $K_a$ ) were in the range described for reference compounds such as pentamidine. Further macromolecular engineering could improve association specificity. The polymer presented no toxicity in cell culture at concentrations of 1.6–100.0  $\mu\text{g}/\text{mL}$  as evaluated both by MTT and real-time monitoring xCELLigence method. These promising results may lay the foundation for a new branch of potential therapeutic agents for DM1.



## INTRODUCTION

Steinert disease, also known as myotonic dystrophy type 1 and dystrophia myotonica type 1 (DM1), is the most common hereditary muscular dystrophy affecting adults, with a prevalence of 1:8000 in Caucasians.<sup>1</sup> DM1 results from a mutation in the dystrophia myotonica protein kinase (DMPK) gene on chromosome 19, position 19q13.32.<sup>2</sup> This mutation is the amplification of the (CTG)<sub>n</sub> trinucleotide repeat located in the 3' untranslated region of the DMPK gene. The disease clinically develops above 50 (CTG) repeats, and the higher the repeat number, the more severe the form. DM1 is a multisystemic disorder, and the symptoms include myotonia (delayed relaxation of muscles), progressive muscle weakness and wasting, insulin resistance, cardiac conduction defects, neuropsychiatric symptoms, gonadal atrophy, and early cataract.<sup>3</sup>

The transcription of the (CTG)<sub>n</sub> triplet expansion in (CUG)<sub>n</sub> repeats, makes DM1 the first recognized example of an RNA-mediated disease. This pathological RNA is retained in the nucleus of affected cells, forming typical double-stranded hairpin structures.<sup>4</sup> The complete physiopathology is still not fully understood but mainly affects two splicing factors: muscle-blind-like protein family (whose MBNL1 is the major one) and CUG-binding protein 1 (CUGBP1). These antagonistic proteins are fundamental in the alternative splicing regulation of pre-mRNAs.<sup>5,6</sup> MBNL1 is sequestered by the

double-stranded hairpin RNA, in typical ribonuclear inclusions (*foci*). The loss of MBNL1 function is directly linked to myotonia<sup>7</sup> and insulin resistance,<sup>8</sup> while on the other hand, the overexpression and stabilization of CUGBP1 could induce muscle wasting.<sup>9</sup>

To this date, no treatment is available for DM1. The present major therapeutic strategies are focused on (i) blocking the (CTG)<sub>n</sub> repeat expansion in the mutated gene, avoiding its transcription,<sup>10</sup> (ii) suppressing or blocking the (CUG)<sub>n</sub> RNA and/or its structural hairpins,<sup>11,12</sup> (iii) overexpressing the sequestered splicing factors,<sup>1,13–15</sup> and (iv) suppressing (CTG)<sub>n</sub> repeat by CRISPR/Cas9 gene editing.<sup>16,17</sup>

So far, antisense technology designed to block the (CUG)<sub>n</sub> repeat on RNA appears to be of limited efficacy (synthetic siRNA,<sup>18</sup> antisense oligonucleotides,<sup>19</sup> and so forth). Small bioactive molecules (low molecular-weight structures or peptoids<sup>20,21</sup>) binding to either the (CTG)<sub>n</sub> expansion on the DMPK gene<sup>10</sup> or to the (CUG)<sub>n</sub> RNA (inhibiting interactions with MBNL1) are considered as potential therapeutic agents. Recently, López-Morató et al.<sup>22</sup> reviewed the current knowledge about the effectiveness of such molecules. Pentamidine (PTMD, Figure 1) was the first

Received: July 3, 2019

Accepted: September 25, 2019

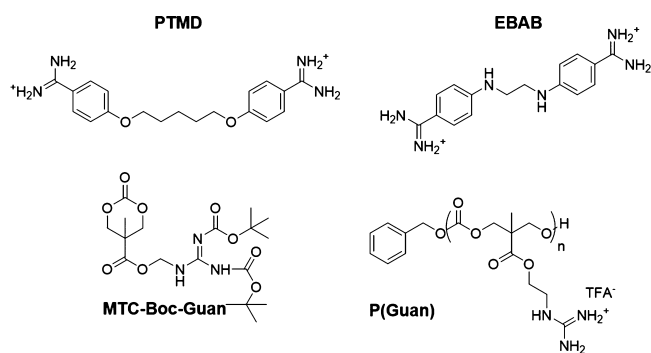


**Figure 1.** Structures of the tested molecules. MTC-Boc-Guan (monomer), P(Guan) (polymer), PTMD, and EBAB.

small molecule tested for this purpose, and it provided good initial results,<sup>23</sup> however hampered by its high toxicity in vivo at therapeutic levels, preventing clinical applicability. Analogues inspired from PTMD structure and mechanism of action were then considered. Indeed, we recently showed the effectiveness of 1,2-ethane bis-1-amino-4-benzamidine (EBAB, Figure 1) that presented a similar activity with a much lower toxicity in vivo than PTMD.<sup>24</sup> In this molecule, the pentyl diether chain of PTMD was replaced by an ethyl diamine chain.

To the best of our knowledge, (synthetic or natural) polymers have not yet been considered as potential therapeutic compounds for DM1 treatment. However, the development of polymers for biomedical applications has been one of the most challenging topics of the past decades, more particularly for drug delivery.<sup>25</sup> Polymers are mostly used as nanocargo vehicles, enhancing the bioaccessibility and efficacy of therapeutic agents, reducing the drug dosage and toxicity. Positively charged polymers were already shown to bind phosphate groups of oligonucleotides through electrostatic interactions.<sup>26–28</sup> Inspired from PTMD, we considered the design of a biocompatible polycation that should lead to an innovative bioactive material, potentially able to interact with (CUG)<sub>n</sub> or (CTG)<sub>n</sub> repeats. The polymer chain could bring improved biocompatibility and biodegradability compared to PTMD. Also, the insertion of different functional groups onto the chain could further modulate its features, such as tailored bioavailability and remanence in the body.

Synthetic aliphatic polycarbonates (APCs) are good candidates for biomedical applications, being biodegradable into nontoxic products<sup>29,30</sup> and biocompatible.<sup>31,32</sup> The main advantage of APCs is their ease of functionalization before or after the polymerization, yielding specifically designed macromolecules able to overcome biological barriers.<sup>33,34</sup> Playing with the type and number of chemical functionalities (e.g., via copolymerization), their electrostatic charge, hydrophobicity, and degradability (amongst others) could be further tuned.

Ring-opening polymerization (ROP) of cyclic carbonates (CCs) is one of the most relevant ways to design APCs.<sup>35</sup> ROP can be achieved using metal-free catalysts,<sup>36</sup> considerably simplifying the costly and time-consuming postpolymerization purification steps. This synthetic pathway avoids residual metals linked to toxicity.<sup>37</sup> Among organic catalysts, the amidine 1,8-diazabicyclo[5.4.0]undec-7-ene (DBU) promotes the ROP of CCs by activation of the initiating alcohol in a *pseudo*-anionic polymerization mechanism. This “super”-base was proven to be noncytotoxic.<sup>38</sup> CC monomers were synthesized based on the route suggested by Pratt and co-

workers,<sup>39</sup> starting from 2,2-bishydroxy(methyl)propionic acid (bis-MPA) (synthetic scheme available in the Supporting Information). Various functions could be attached through this monomer synthesis, taking into account their possible interaction or DBU catalyst deactivation during polymerization.

Inspired by the PTMD structure, and by several investigations of polymer–oligonucleotide interaction,<sup>40–42</sup> we decided to prepare CC monomers carrying guanidine functions (MTC-Boc-Guan, Figure 1). As guanidines could interact during the ROP process, they were protected using *tert*-butyloxycarbonyl (Boc) groups. The deprotection was done in a postpolymerization treatment before use. The resulting charged polycation (P(Guan), Figure 1) could interact with the negative charges of the oligonucleotides.

We first wanted to evaluate the interaction between the P(Guan) polymer and the (CUG)<sub>n</sub> repeat RNA by studies in vitro. Potentially active ligands in DM1 are usually identified through screening techniques by investigating nucleic acid (DNA/RNA)-drug interactions using target probes with pathological triplet repeat expansions. Electrophoretic mobility shift assay and fluorescence microscopy are often used for such purposes.

Recently, capillary electrophoresis (CE) has been successfully implemented in the study of various types of interactions,<sup>43–45</sup> but it is still underused for nucleic acid–ligand interaction assessment.<sup>46</sup> Among various electromigration techniques available for such interaction studies, affinity CE (ACE) is particularly useful. It implies the use of a pair of compounds, acting arbitrarily as ligands or analytes. The ligand is added to the running buffer, constituting a pseudostationary phase, whereas the analyte is injected as a sample. The dynamic interaction between the two will decrease the electrophoretic mobility of the analyte and consequently its migration time. The binding constant is determined based on the change in the migration time as a function of ligand concentration. A main advantage of ACE in comparison with other affinity-based liquid chromatographic techniques is the small volume requirements of both the ligand and the analyte, which significantly reduces costs and widens product accessibility. Furthermore, the high separation efficiency enables the measurement of binding constants even for low-purity analytes. The possibility of ACE automation is another valuable asset for the screening of large libraries of compounds.<sup>46,47</sup>

In a previous study, we demonstrated the usefulness of ACE for the screening of small ligands in DM1.<sup>24</sup> The developed method confirmed the high affinity of PTMD and of its novel synthetic analogue, EBAB, toward the (CUG)<sub>50</sub> probe. Nevertheless, a repetition of 50 CUG is borderline for the clinical manifestations of DM1, and it is not fully representative for the disease. Furthermore, Coonrod et al.<sup>10</sup> recently proved that PTMD may have its therapeutic effect by acting on DNA (CTG)<sub>n</sub> repeats, inhibiting transcription. On the basis of these findings, we propose to improve the disease model by synthesizing longer RNA targets ((CUG)<sub>95</sub>) and extending the tests to DNA (CTG)<sub>95</sub> targets as well. Both pure (CTG)<sub>95</sub> fragment and (CTG)<sub>95</sub> contained in a linearized plasmid were considered as DNA targets. The previously developed ACE method was used for testing these “DM1-like” probes.

Like for PTMD, the cellular toxicity of P(Guan) remained a key parameter to assess. Its positive charge could induce

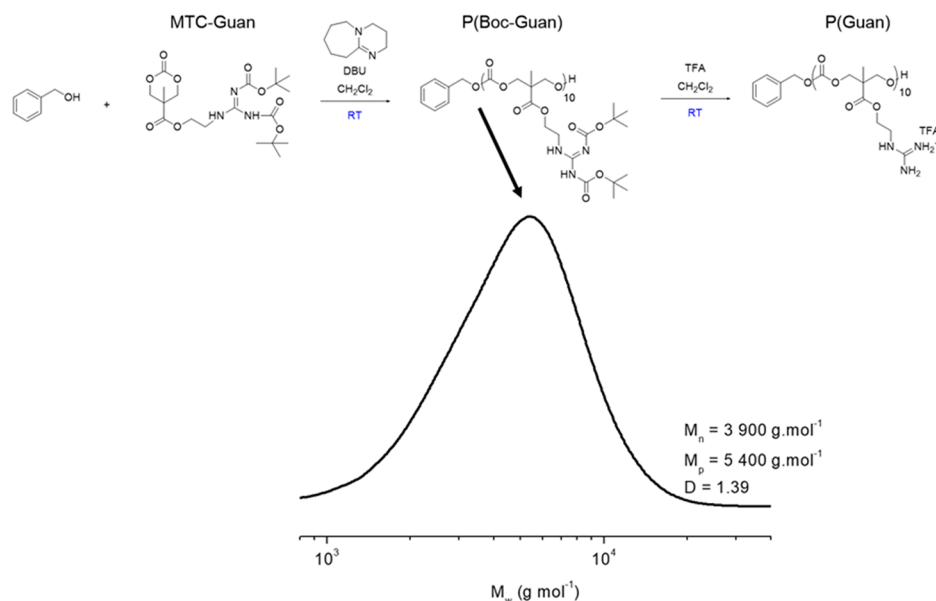


**Figure 2.** Synthesis pathway of the P(Guan) polycation and SEC chromatogram of P(Boc-Guan) after purification by precipitation in *iso*-propanol from DCM before deprotection. Molar masses are equivalent to polystyrene standards.

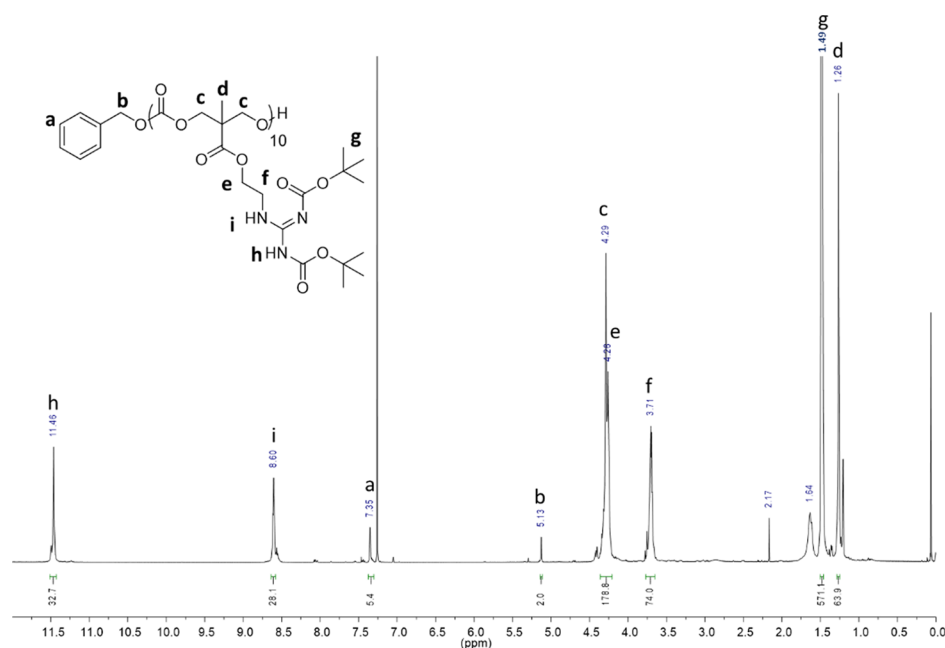


**Figure 3.** <sup>1</sup>H NMR of P(Boc-Guan) in CDCl<sub>3</sub> after purification by reverse precipitation in cold *iso*-propanol, confirming the Boced guanidine functions carried by the aliphatic backbone.

interaction with membranes causing their lysis. In that regard, Cho et al.<sup>48</sup> proved the strong effect of a polymer charge density on hemagglutination. On the other hand, Frère et al.<sup>49,50</sup> proved the noncytotoxicity of polycarbonate copolymers carrying guanidinium functions (by classical colorimetric test able to assess cell viability and hemocompatibility assays). In the present study, we evaluated cytotoxicity both by MTT assay (endpoint label-based viability readout) and real-time monitoring of cell viability by the xCELLigence system.

Considered as a relevant preliminary test for the assessment of polymer toxicity and biocompatibility, MTT assay is based on the metabolic reduction of tetrazolium salt into formazan crystals. Once dissolved in dimethyl sulfoxide (DMSO), this purple compound can be quantified by spectrophotometry and

its concentration reflects the number of metabolically active cells. The xCELLigence system allows for continuous measurement of impedance variations in the function of cell growth or death, using culture plates containing gold microelectrodes.<sup>51</sup>

To sum up, this research work aimed to evaluate in a first trial the ability of a bioactive polymer to act as a therapeutic agent in DM1. As a proof of concept, the binding constants between an aliphatic polycarbonate carrying guanidinium functions (P(Guan)) and DNA (CTG)<sub>95</sub>/RNA (CUG)<sub>95</sub> were measured using an ACE technique and compared to reference compounds (namely PTMD and EBAB). The cytotoxicity of the polymeric material was evaluated in parallel via MTT assays and real-time monitoring xCELLigence.

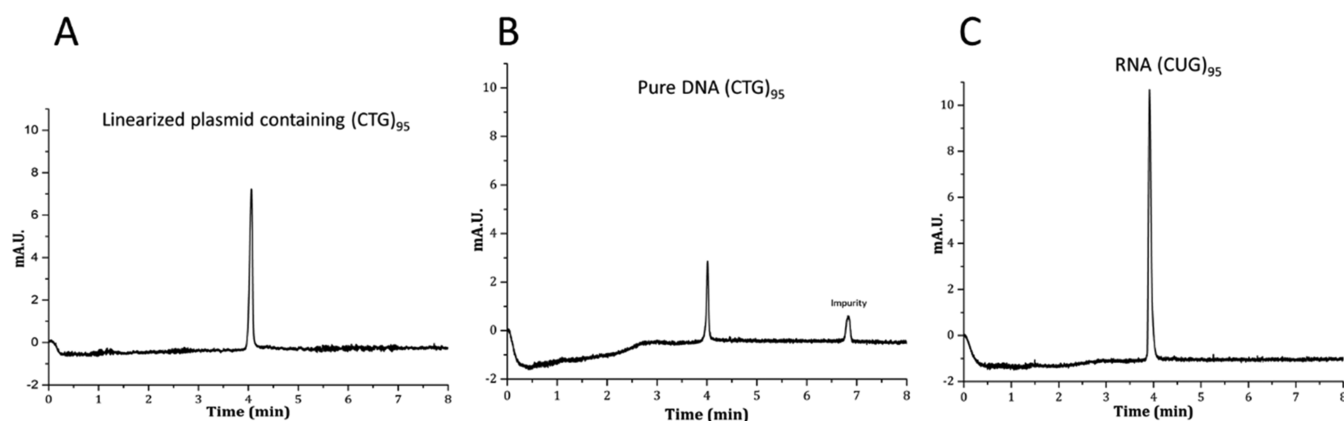


**Figure 4.** Electropherograms of: (A) linearized plasmid containing  $(CTG)_{95}$ ; (B) purified  $(CTG)_{95}$  DNA fragment; and (C) purified  $(CUG)_{95}$  RNA. Conditions: 50 mM HEPES buffer, pH = 7.4; sample plug 50 mbar  $\times$  5 s. Fused silica capillary dynamically coated with PEO.  $L_{tot}$  = 40 cm,  $L_{eff}$  = 31.5 cm, potential:  $-15$  kV; nucleic acid targets: 200  $\mu$ g/mL.

## RESULTS AND DISCUSSION

**Polymer Synthesis.** As a novel research strategy for DM1 treatment, we synthesized an aliphatic polycarbonate carrying guanidinium functions with the aim to evaluate this polycation binding to DNA/RNA model probes with amplified CTG/CUG triplet repeats. The CC monomer carrying protected (Boced) guanidine was prepared starting from bis-MPA, following a synthetic route inspired from Pratt et al.<sup>39</sup> In this route, safer ethyl chloroformate and triethylamine (TEA) replaced triphosgene for performing the ring closure (synthetic scheme and protocol available in the [Supporting Information](#)). The pure monomer obtained was subsequently dried before its use for polymerization (MTC-Boc-Guan, yield = 60%,  $^1H$  NMR available in the [Supporting Information](#), Figure S4).

The macromolecular chain was synthesized via ROP, organo-catalyzed by DBU, and initiated by benzyl alcohol. We aimed for a short homopolymer with 10 repeat units (P(Boc-Guan), [Figure 2](#)). After quenching of the polymerization reaction, the material was purified by precipitation in *iso*-propanol from concentrated solution of dichloromethane (DCM). The polymer was characterized by size exclusion chromatography (SEC, [Figure 2](#)) and  $^1H$  NMR spectroscopy ([Figure 3](#)). The purification efficacy (elimination of small molecules and oligomers) was highlighted on the SEC profile ([Supporting Information](#), Figure S5).

The SEC chromatograms depicted a monomodal molar mass distribution with a dispersity index of 1.39 and a molar mass of 3.9 kDa (equivalent to polystyrene standards, [Figure 2](#)). This high dispersity index, contrary to the ones usually observed for APCs obtained by ROP (around 1.2), indicated a poor polymerization control. Investigation of possible side-reactions led to the identification of undesired initiation from other compounds than benzyl alcohol (e.g., water traces). Therefore, the polymer batch contained several macromolecular populations of lower molar mass than targeted.

The  $^1H$  NMR spectrum after purification confirmed the presence of protected guanidine functions all along the polymer backbone, as well as the absence of residual catalyst or monomers ([Figure 3](#)). Setting the integration of the ethyl of BzO-peaks equal to 2 (Ph-CH<sub>2</sub>-O-,  $\delta$  = 5.13 in CDCl<sub>3</sub>) was chosen for the calculation of the repeat unit number (degree of polymerization). Polymer peak integrations were thus calibrated in accordance with the benzyl alcohol peaks. After calculation, the  $^1H$  NMR data indicated a polymer carrying 30

units of Boced guanidine, with a subsequent molar mass of 12 kDa. Those figures were largely superior to SEC results and confirmed the presence of multiple macromolecular species in the polymer batch. As no other initiator was detected on  $^1H$  NMR, we suspected that polymerization had started from a diol corresponding to the opened monomer form.

Despite a higher dispersity and the lack of end-chain fidelity, we obtained a short oligomer of polycarbonate carrying lateral guanidines. We estimated that this P(Boc-Guan) was suitable for a proof of concept study. Nevertheless, the polymerization control should be improved for future experiments. To be able to interact with oligonucleotides, P(Boc-Guan)'s guanidine functions were deprotected using trifluoroacetic acid (TFA). The deprotection effectiveness was confirmed by  $^1H$  NMR, with the disappearance of Boc group signals at  $\delta$  = 1.49 ppm ([Supporting Information](#), Figure S6).

**Application of the ACE Method to the Newly Synthesized DM1-like Probes.** We previously used ACE to investigate the binding of PTMD and synthesized derivatives on a commercially available  $(CUG)_{50}$  RNA probe.<sup>24</sup> However, as mentioned in the introduction, a  $(CUG)_{50}$  array is not completely representative of DM1 heterogeneity. In order to better model the pathology, we used conventional biomolecular techniques such as transcription *in vitro* to obtain  $(CUG)_{95}$  RNA, and purification of a  $(CTG)_{95}$  DNA restriction fragment from a plasmid amplified in *Escherichia coli*. To evaluate nonspecific interactions, we also used the whole linearized plasmid. The three nucleic acid probes were quality checked by agarose gel electrophoresis (data not shown).

In the first set of experiments, the three nucleic acid probes were run in CE in identical conditions to assess their mobilities in the absence of a ligand ([Figure 4](#)).

In the second set of experiments, sequential ACE assays were performed for each nucleic acid probe with increasing concentrations of the ligand (PTMD or EBAB, in the range of 0–200  $\mu$ M) added into the running buffer. The migration times were processed using nonlinear regression as the fitting procedure ([Supporting Information](#), Figures S7 and S8), offering better accuracy and precision compared to linear regression.<sup>52–54</sup>

The binding constant ( $K_a$ ) of PTMD with  $(CUG)_{95}$  RNA was similar to, although, as expected, slightly higher than the one previously obtained with the  $(CUG)_{50}$  RNA probe ([Table](#)

1,  $K_a = 16.30 \times 10^3 \text{ M}^{-1}$ ). This confirmed the adequacy of the new RNA probe as a DM1-model. The smaller affinities of

**Table 1. Binding Constants of Reference Compounds (PTMD and EBAB) and The P(Guan) Polycation Observed by ACE with Probes Harboring Short (50) or Long (95) Triplet Expansions**

	RNA (CUG) <sub>50</sub> <sup>24</sup> $K_a$ [ $\times 10^3 \text{ M}^{-1}$ ]	RNA (CUG) <sub>95</sub> $K_a$ [ $\times 10^3 \text{ M}^{-1}$ ]	linearized plasmid containing (CTG) <sub>95</sub> $K_a$ [ $\times 10^3 \text{ M}^{-1}$ ]	DNA (CTG) <sub>95</sub> $K_a$ [ $\times 10^3 \text{ M}^{-1}$ ]
PTMD	14.78	16.30	8.82	4.60
EBAB	12.09	53.42	9.96	9.56
P(Guan)	<sup>a</sup>	22.50	36.83	2.45

<sup>a</sup>Not measured.

PTMD toward the plasmid ( $K_a = 8.82 \times 10^3 \text{ M}^{-1}$ ) and purified (CTG)<sub>95</sub> DNA fragment ( $K_a = 4.60 \times 10^3 \text{ M}^{-1}$ ) indicated a preferential interaction with the RNA probe. In addition, an almost two-fold higher binding constant was found for (CTG)<sub>95</sub> DNA within the plasmid as compared with the purified DNA fragment indicating the presence of additional, nonspecific interactions with other parts of the plasmid sequence.

The nontoxic PTMD derivative EBAB presented a similar affinity as PTMD for the (CUG)<sub>50</sub> RNA probe (Table 1). In the present study, EBAB bound the longer (CUG)<sub>95</sub> RNA probe with about four-fold higher  $K_a$  ( $53.42 \times 10^3 \text{ M}^{-1}$ ), than the shorter (CUG)<sub>50</sub> RNA. The affinity was thus higher for EBAB than PTMD in the same conditions. Moreover, among the two reference ligands, EBAB probably showed the highest specificity in the interaction with (CTG)<sub>95</sub> DNA, based on the similar  $K_a$  obtained with both the plasmid ( $K_a = 9.96 \times 10^3 \text{ M}^{-1}$ ) and purified DNA ( $K_a = 9.56 \times 10^3 \text{ M}^{-1}$ ) fragment.

Affinity studies performed with P(Guan) polycation revealed a binding constant to (CUG)<sub>95</sub> RNA slightly higher ( $K_a =$

$22.50 \times 10^3 \text{ M}^{-1}$ ) than PTMD, and about half the  $K_a$  recorded for EBAB. Also, P(Guan) demonstrated a strong interaction with the linearized (CTG)<sub>95</sub> plasmid, yielding a 4-fold higher  $K_a$  ( $36.83 \times 10^3 \text{ M}^{-1}$ ) than reference compounds. On the other hand, P(Guan) interaction with the purified (CTG)<sub>95</sub> DNA fragment yielded a 15-fold lower  $K_a$  value ( $2.45 \times 10^3 \text{ M}^{-1}$ ), indicating additional nonspecific interactions with the plasmid backbone.

**Cytotoxicity Evaluation.** As the positive charges all along the P(Guan) polymer backbone could induce interaction with phospholipids and disruption of cell membranes, its potential cytotoxicity was investigated. We used HeLa cell cultures and complementary techniques to evaluate live cell numbers, i.e., MTT assay (endpoint label-based) and impedance-based real-time monitoring cytotoxicity assay (xCELLigence system).

To the best of our knowledge, no experimental protocol has been reported on the evaluation of polymers by the xCELLigence method. To make sure that the studied polymer did not alter results and the skew cell index measure by a role on the measured impedance, P(Guan) was incubated in the absence of cells at the highest tested concentration (100  $\mu\text{g}/\text{mL}$ ) in plate wells. Even if the polymer itself gave a slightly positive value, its impact was negligible and considered as not interfering (profile available in the Supporting Information, Figure S9).

In the xCELLigence protocol, 24 h HeLa cell proliferation was followed by exposure to P(Guan). The important peak observed 3–5 h after treatment in the cell index profiles is common and can be ascribed to manipulation stress, as it is observed for nontreated cells as well (Figure 5, green curve).

The cytotoxicity data obtained by either technique were in good agreement (Figure 5), indicating no statistically significant cytotoxicity of P(Guan) in the tested range of concentrations.

## MATERIALS AND METHODS

**Materials.** 2,2-Bis(hydroxymethyl)propionic acid (bis-MPA) (98%, Aldrich); potassium hydroxide (KOH) (90%,

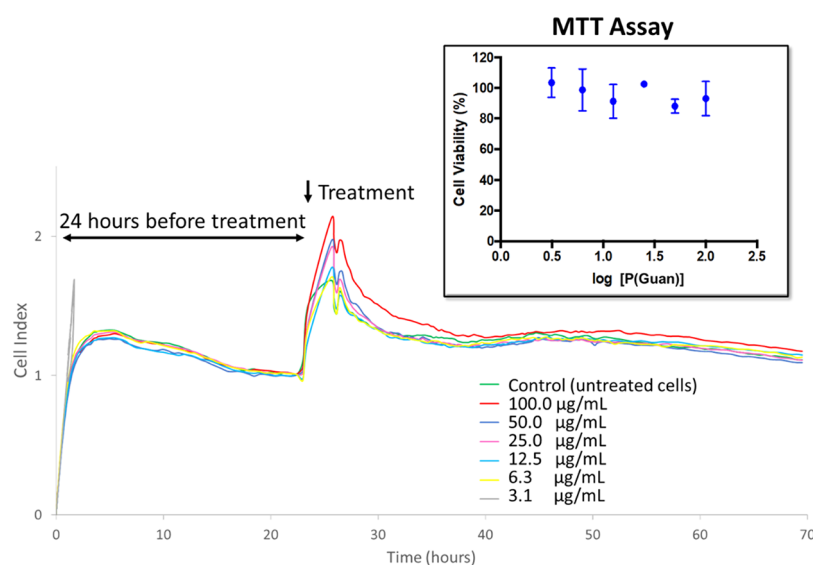


**Figure 5.** Cell viability performed by MTT assay and real-time monitoring (xCELLigence) on HeLa cells in the presence of P(Guan). In MTT, cell viability was expressed as % (in comparison to the control = nontreated cells). In xCELLigence, cell index derived from impedance measurements. After 24 h of incubation, HeLa cells were treated with the indicated concentrations of P(Guan) added to the culture medium (see Methods). Control curve (green line) represents nontreated cells.

Aldrich); benzyl bromide (98%, Aldrich); *N,N*-dimethylformamide (DMF) (anhydrous, 99.8%, Aldrich); ethyl acetate (VWR); anhydrous  $\text{MgSO}_4$  (Amresco); ethyl chloroformate (97%, Alfa Aesar); palladium on activated charcoal ( $\text{Pd}_{10\%}/\text{C}$ , Aldrich); calcined diatomaceous earth (Celite 545, Acros); oxalyl chloride (98%, Alfa Aesar); 1,3-diBoc-2-(2-hydroxyethyl)guanidine (>96%, Aldrich); weakly acidic alumina (Aldrich); chloroform ( $\text{CHCl}_3$ , >99.8%, Aldrich); *iso*-propanol (VWR); TFA (99% Aldrich); phosphorus pentoxide ( $\text{P}_2\text{O}_5$ , VWR); HEPES (Sigma-Aldrich); poly(ethylene oxide) (PEO, 200 K, Sigma-Aldrich); and pentamidine isethionate and imidazole (PTMD, Sigma-Aldrich) were used as received.

TEA (> 99%, Aldrich) was dried and stored over barium oxide ( $\text{BaO}$ , 97%, VWR). When dried solvents were required, DCM, tetrahydrofuran (THF), and toluene were dried using a MBraun Solvent Purification System (model MB-SPS 800) equipped with alumina drying columns. Molecular sieves (4 Å) were washed three times using THF and dried overnight under vacuum at 80 °C, then activated overnight under vacuum at 200 °C. Sieve beads were stored in a glove box. Benzoic acid was recrystallized from toluene, dried under vacuum, and stored in a glove box. All materials used for polymerization were properly dried and stored in a glove box before use. Benzyl alcohol ( $\text{BzOH}$ , 97%, Sigma) was dried over  $\text{CaH}_2$  for 48 h at room temperature (RT), distilled under reduced pressure, and stored in a glove box. 1,8-Diazabicyclo [5.4.0]undec-7-ene (DBU, 99%, Fluka) was dried over  $\text{BaO}$  for 48 h at RT, then distilled under reduced pressure, and stored in a glove box. All materials used for polymerization were properly dried and stored in a glove box before use. EBAB was synthesized as described.<sup>55</sup> Ultrapure deionized water (18.2 MΩ) was used for the preparation of all working solutions and buffers (Milli-Q Reference Water Purification System, Merck). A 50 mM HEPES (pH 7.4) buffer solution was used for the dissolution of the ligands (stored at -4 °C). Daily fresh aliquots were prepared from (~1 mM) ligand stock solution in HEPES buffer (stored at -20 °C). All working solutions were passed through 0.2 μm pore size Spartan syringe filters (Whatman) and degassed by sonication for at least 5 min before use. For the dynamic coating of the bare fused silica capillary, a PEO coating solution was used as previously described.<sup>24</sup>

**Synthesis. Nucleic Acid Probes.** The nucleic acid targets were synthesized and purified in our laboratory. In brief, the RNA target was synthesized using an in vitro transcription kit (HiScribe SP6 RNA Synthesis Kit, New England Biolabs). The template plasmid, containing the (CTG)<sub>95</sub> insert (provided by Dr. Denis Furling, Institute of Myology, Paris, France) was linearized using *Hind*III (Invitrogen by Thermo Fisher Scientific AnzaTM) restriction enzyme before in vitro transcription.

The plasmid containing the (CTG)<sub>95</sub> DNA target was amplified after bacterial transformation. It was extracted using the ZymoPURE Plasmid Gigaprep kit (Zymo Research). A part of the produced plasmid was linearized with *Hind*III, purified by ethanol precipitation, and used as such for the ACE experiments.

The second part of the plasmid preparation was cut with *Hind*III and *Xho*I to release the (CTG)<sub>95</sub> DNA fragment. The digestion products were separated by preparative gel electrophoresis on 1% agarose gel (using an in-house built system). A thin gel lane was cut on either side of the gel, stained with

ethidium bromide, and visualized under UV light to identify the (CTG)<sub>95</sub> DNA fragment. The nonstained central gel part containing the fragment of interest was then cut out and DNA extracted from the agarose gel slice using an in-house electroelution system. Finally, the DNA (CTG)<sub>95</sub> fragment was reprecipitated with ethanol from the extraction buffer.

**CC Monomers.** All steps leading to the carboxylic acid CC (MTC-COOH) are available in the Supporting Information, including the <sup>1</sup>H NMR spectra (Figures S1–S3).

All of the next steps were done under nitrogen flow. MTC-COOH (1 g, 1 equiv) was dissolved in 45 mL of anhydrous THF with 3 drops of DMF (catalyst). A solution of 1.607 mL of oxalyl chloride (3 equiv) in 5 mL of anhydrous THF was added dropwise at 0 °C and maintained under stirring for 1 h at RT. Volatile solvents were then removed under vacuum. Anhydrous THF (50 mL) was added and similarly evaporated to eliminate any trace of contaminants. The as-prepared acyl chloride was dissolved in 50 mL of anhydrous THF. A solution of 0.828 mL of TEA (0.95 equiv), 1.8 g of 1,3-diBoc 2-(2-hydroxyethyl) guanidine (0.95 equiv), and 5 mL of THF were added dropwise at 0 °C. The reaction was stirred for 3 h at RT. Residual salts were then filtered off and volatiles were removed under vacuum. The crude product was dissolved in chloroform (ca. 10 mL) and filtered through a weakly acidic aluminum oxide bed (ca. 1 cm height). The column was then washed with chloroform excess (ca. 100 mL). The solvent was finally eliminated under vacuum to yield a white powder of 1,3-diBoc-2-(2-hydroxyethyl)guanidine-5-methyl-2-oxo-1,3-dioxane-5-carboxylate (MTC-Boc-Guan, yield = 60%). The product was dried overnight under vacuum, at RT, and in the presence of  $\text{P}_2\text{O}_5$  (a water-catching agent). It was then stored under protective atmosphere ( $\text{N}_2$ ) in a glove box. <sup>1</sup>H NMR confirmed the absence of interfering contaminant (Figure S4).

**Ring-Opening Polymerization.** All of the products (monomer, catalyst, solvent, and quench agent) were carefully dried prior to use as described in the Materials section. The polymerization was done in a glove box ( $\text{N}_2$  atmosphere) containing flame-dried glassware. In a vial, a solution of 200 mg of MTC-Boc-Guan monomer (10 mol equiv) in 400 μL of DCM was prepared and left under stirring with molecular sieves (monomer initial concentration = 1 M). In another vial, a solution of 6.8 μL of DBU (1 mol equiv) and 4.9 μL of  $\text{BzOH}$  (1 mol equiv) in 49 μL of DCM was prepared and maintained under stirring with molecular sieves. The monomer solution was added to the catalyst/initiator solution, and the polymerization mix was stirred until maximal conversion (about 1 h). The polymerization was then quenched with benzoic acid (5 mg/mg of DBU). The polymer was concentrated and purified by multiple reverse precipitations in cold *iso*-propanol to yield P(Boc-Guan) as a colorless polymer. The material was dried overnight under vacuum (RT) prior to analysis.

**Postpolymerization Deprotection of Pendant Boced Guanidine Functions.** P(Boc-Guan) (100 mg) was dissolved in 4 mL of anhydrous DCM. TFA (1.2 mL) was slowly added and left under stirring for 1 h 30 min at RT until the solution became cloudy. Volatiles were eliminated under vacuum, and the deprotected polymer was dried overnight under vacuum (RT) prior to analysis and use.

**Methods. Polymer Characterization.** SEC was performed in THF (98:2; v/v) at 35 °C using an Agilent 1200 liquid chromatography system equipped with a degasser, an isocratic pump, an autosampler (200 mL loop), a set of two PLgel 10

mm MIXED-B ultrahigh-efficiency columns using a differential refractive index, and a UV–vis detector. A 100 mL sample solution in an eluent (concentration 0.1% w/v) was injected. Molecular weight and molecular weight distribution were calculated with reference to polystyrene standards (Polymer Laboratories).

$^1\text{H}$  NMR spectra were recorded in  $\text{CDCl}_3$  or in  $\text{DMSO}-d_6$ , with tetramethylsilane as an internal standard, at RT with a Bruker AMX-500 spectrometer operating at 500 MHz, equipped with a BBO probe. Spectra were obtained over 32 scans (sample concentration 10 mg/0.6 mL).

**PEO-Coated CE.** The PEO-coated capillary was prepared as described in the previous works.<sup>24,56</sup> The experiments were performed using an Agilent G1600 CE system (Agilent Technologies), and the samples were injected hydrodynamically (50 mbar  $\times$  5 s). The bare fused silica capillary was acquired from Polymicro Technologies. All capillaries had an internal diameter of 50  $\mu\text{m}$ , an external diameter of 365  $\mu\text{m}$ , and total length of 40 cm. Detection was performed with the built-in diode-array detector at 260 nm.

**Binding Constant Evaluation.** The samples were first run in 50 mM HEPES, pH 7.4, and subsequently in the same buffer with increasing concentrations (from 0 up to 200  $\mu\text{M}$ ) of the tested ligand.<sup>24</sup>

The analyses were performed in triplicate ( $n = 3$ ) at a separation voltage of  $-15$  kV, and the detection was done at the characteristic UV absorption maxima of the DNA/RNA probes (260 nm). Each ACE assay lasted 14 min with a total run time of 31 min (including the preconditioning step). At each ligand concentration, the analyte electrophoretic mobility was calculated based on its recorded migration time using formula 1.

$$\mu = L_t \times L_{\text{eff}} / (t_m \times V) \quad (1)$$

where  $L_t$  is the total capillary length,  $L_{\text{eff}}$  is the effective capillary length (the length up to the detector),  $t_m$  is the analyte migration time, and  $V$  is the separation voltage.

The binding constant for each ligand was assessed using nonlinear regression, based on eq 2<sup>57</sup>

$$\Delta\mu = K_b \times (\mu_{\text{max}} - \mu_0) \times [L / (1 + K_b \times L)] \quad (2)$$

where  $\Delta\mu$  is the difference in the electrophoretic mobility for the analyte with either no ligand or a given ligand concentration in the buffer,  $L$  is the ligand concentration in the buffer,  $K_b$  is the binding constant, and  $\Delta\mu_{\text{max}}$  is the maximum difference in electrophoretic mobility (in the absence or presence of a ligand in the buffer),  $\mu_0$  is the electrophoretic mobility of the analyte with no ligand in the buffer, and  $\mu_{\text{max}}$  is the mobility of the analyte at the maximum ligand concentration, above which there is no more mobility change.

For data analysis and nonlinear regression fitting, Origin 2016 (OriginLab, trial version) was used.

**Polymer Cytotoxicity Evaluation.** The synthesized and deprotected P(Guan) polymer was assessed for toxicity in HeLa cells by an endpoint (MTT assay) and a dynamic (xCELLigence) method.

**Cell Culture.** HeLa cells (cervix adenocarcinoma; ATCC # CCL-2) were cultured in DMEM + GlutaMAX growth medium (Gibco, Fisher Scientific) supplemented with 10% fetal bovine serum (FBS South American (CE), Gibco, Fisher Scientific) and 1% penicillin–streptomycin mixture (PenStrep, Lonza). Culture plates were maintained in the incubator under

a humid atmosphere (37  $^\circ\text{C}$ , 5%  $\text{CO}_2$ ). A stock solution of polymer P(Guan) was prepared (10 mg/mL) in distilled water.

**MTT Assay.** The cell viability was evaluated using thiazolyl blue tetrazolium bromide (Sigma-Aldrich) assay, which indicates the metabolic activity of cells. The experiment was performed in 96-well microplates seeded at a density of 5000 HeLa cells per well, and placed in the incubator under a humid atmosphere (37  $^\circ\text{C}$ , 5%  $\text{CO}_2$ ). The polymer stock solution was diluted in medium (DMEM + 10% FBS + 1% PenStrep) to reach final concentrations ranging from 1.6 to 100  $\mu\text{g}/\text{mL}$ .

After 24 h, 200  $\mu\text{L}$  of the culture medium was discarded from each well and replaced by 200  $\mu\text{L}$  of each polymer dilution ( $n = 3$ ). Plates were then placed back in the incubator for 24 h. Cells were then washed three times with phosphate-buffered saline (PBS, Gibco, Fisher Scientific) and 200  $\mu\text{L}$  of the thiazolyl blue tetrazolium bromide solution (0.5 mg/mL in PBS, pH = 7.4) was added to each well and left to incubate for a further 4 h at 37  $^\circ\text{C}$ . The MTT reagent was thereafter removed and formazan crystals formed in viable cells were dissolved in 100  $\mu\text{L}$  of DMSO ( $\geq 99\%$ , Sigma-Aldrich). Microplates were shaken, and each well absorbance was measured at 570 nm (Thermo Labsystems Multiskan Ascent microplate reader).

**Real-Time Monitoring of Cell Viability Using xCELLigence.** The experiments were performed on an xCELLigence RTCA SP device (ACEA Biosciences). During the first series of experiments, 100  $\mu\text{L}$  of DMEM + GlutaMAX growth medium supplemented with 10% FBS and 1% penicillin–streptomycin mixture was added in each well of the device VIEW 16 E-Plate.<sup>58</sup> A background measure of impedance, converted into a cell index, was then performed. Each well was seeded with 5000 HeLa cells suspended in 200  $\mu\text{L}$  of growth medium. After gentle mixing, cells were allowed to sediment for 30 min at RT, and then the E-plate was put back in the RTCA analyzer. Cells were cultured for approximately 24 h, and an impedance measurement was recorded every 15 min and converted into cell index, which is representative of the cell viability.

The polymer stock solution was diluted in culture medium to reach final concentrations ranging from 3.1 to 100  $\mu\text{g}/\text{mL}$ .

After 24 h, 100  $\mu\text{L}$  of the culture medium was discarded and replaced with 100  $\mu\text{L}$  of each polymer dilution in the culture medium (between 0 and 200  $\mu\text{M}$ ,  $n = 3$ ). Plates were put back in the RTCA analyzer and the cell index was monitored after treatment for a further 48 h.

Impedance monitoring of polymer solutions without cells was also performed to evaluate whether these macromolecules did not contribute by themselves to the electrical impedance increase.

## CONCLUSIONS

In the present study, we investigated by ACE two classes of compounds (pentamidines and a polycation) for their binding affinity to nucleic acids harboring triplet repeat arrays typical of DM1. Compared to our previous publication,<sup>24</sup> longer triplet repeat arrays (95 triplets instead of 50), more representative of the pathology, were used: linearized plasmid containing (CTG)<sub>95</sub> array, purified (CTG)<sub>95</sub> DNA fragment, and (CUG)<sub>95</sub> RNA. Those longer “DM1-like” probes were first shown by ACE to bind two reference compounds (PTMD and EBAB) with high affinity. A better binding specificity was observed for EBAB as compared to PTMD and confirmed a higher affinity of both compounds toward (CUG)<sub>95</sub> RNA versus (plasmid and purified fragment) (CTG)<sub>95</sub> DNA. This

strong interaction, in addition to its ability to decrease pathological (CUG)<sub>50</sub> RNA foci in cell nuclei,<sup>24</sup> again confirmed EBAB as a candidate for further investigations in correcting the DM1 pathological phenotype (rescue of abnormal RNA splicing in cell culture and DM1 model in vivo).

For the first time in the investigations of potential therapeutic strategies for DM1, a polycation P(Guan) was designed based on an aliphatic polycarbonate carrying guanidinium functions, prepared by organo-catalyzed ROP ( $M_n = 3900 \text{ g mol}^{-1}$ ;  $D = 1.39$ ). Even if the polymerization process did not perform as expected in terms of control, the obtained product could be used for a proof of concept experiment. Complementary cytotoxicity tests (MTT assay and xCELLigence method) both proved the nontoxicity of P(Guan) in the range of tested concentrations (1.6–100.0  $\mu\text{g/mL}$ ).

P(Guan)'s affinity for "DM1-like" probes was assessed by ACE and compared to the two reference molecules. The binding of P(guan) to (CUG)<sub>95</sub>, the most representative nucleic acid probes in terms of DM1 pathology, is noteworthy ( $K_a = 22.50 \times 10^3 \text{ M}^{-1}$ ). This obtained  $K_a$  was slightly higher than PTMD ( $16.30 \times 10^3 \text{ M}^{-1}$ ), and about half of the  $K_a$  recorded for EBAB ( $53.42 \times 10^3 \text{ M}^{-1}$ ). On the other hand, P(Guan) interaction with the purified DNA (CTG)<sub>95</sub> ( $K_a = 2.45 \times 10^3 \text{ M}^{-1}$ ) was weaker than with the linearized plasmid ( $K_a = 36.83 \times 10^3 \text{ M}^{-1}$ ), suggesting the occurrence of additional nonspecific interactions with the plasmid DNA (CTG)<sub>95</sub>.

As specificity for the triplet repeat array is the ultimate goal in the strategy, these initial findings should be evaluated in the light of interactions with nontargeted DNA sequences. Several probe templates should be tested, containing triplet arrays other than (CTG)<sub>n</sub> or (CUG)<sub>n</sub>. Also, it would be interesting to compare  $K_a$  obtained with plasmids having different length of (CTG)<sub>n</sub>, including a nonpathologic array, e.g., (CTG)<sub>15</sub>.

Considering the great versatility of polymer design, many possibilities are open in terms of macromolecular engineering. For instance, further optimizing the type of cations (e.g., morpholino instead of guanidinium) and tailoring the architecture (e.g., using spacing agents to "dilute" the cationic charge) hold great promise in the improvement of interaction specificity. The fine tuning of the repetitive units on the polymer in better modeling specific reference molecules (e.g., EBAB) should also lead to tailor-made polymeric materials.

Finally, the high binding affinity of P(Guan) to (CUG)<sub>95</sub> warrants further studies to complete the biological characterization in the DM1 context. The biodegradability profile of the polymer backbone and its influence on activity and toxicity should be investigated.

Indubitably, if we confirm the potential activity of our polymeric or nonpolymeric candidates, we have to evaluate the permeation performances across biological barriers. Once the in vitro interaction is confirmed, the next step consists of performing in vivo assays to evaluate the concrete ability of our APCs to become a therapeutic strategy.

## ■ ASSOCIATED CONTENT

### ● Supporting Information

The Supporting Information is available free of charge on the ACS Publications website at DOI: 10.1021/acsomega.9b02034.

Syntheses of monomer; <sup>1</sup>H NMR in CDCl<sub>3</sub> of Diol-Bn, benzyl cyclic carbonate (MBC), and monomer cyclic carbonate (MTC-Boc-Guan); <sup>1</sup>H NMR in DMSO-*d*<sub>6</sub> of carboxylic acid cyclic carbonate (MTC-COOH); SEC profile of P(Boc-Guan); <sup>1</sup>H NMR in DMSO-*d*<sub>6</sub> of the polycation P(Guan) after deprotection of guanidine functions; series of electropherograms of (CUG)<sub>95</sub> RNA; nonlinear regression fitting for (CUG)<sub>95</sub> RNA versus PTMD; and assay with xCELLigence equipment (PDF)

## ■ AUTHOR INFORMATION

### Corresponding Authors

\*E-mail: stephanie.hambye@umons.ac.be (S.H.).

\*E-mail: bertrand.blankert@umons.ac.be (B.B.).

### ORCID

Ede Bodoki: 0000-0003-4667-2286

Bertrand Blankert: 0000-0002-6667-7677

### Author Contributions

The manuscript was written through contributions of all authors. All authors have given approval to the final version of the manuscript.

### Funding

Alexandra Baroni is a F.R.S-FNRS Research Fellow.

### Notes

The authors declare no competing financial interest.

## ■ ACKNOWLEDGMENTS

We thank Dr. Denis Furling (Institute of Myology, Paris, France) for providing the template plasmid containing the (CTG)<sub>95</sub> insert. We thank the FSHD Global research Foundation for its financial support.

## ■ REFERENCES

- (1) Foff, E. P.; Mahadevan, M. S. Therapeutics Development in Myotonic Dystrophy Type 1. *Muscle Nerve* **2011**, *44*, 160–169.
- (2) Harley, H. G.; Walsh, K. V.; Rundle, S.; Brook, J. D.; Sarfarazi, M.; Koch, M. C.; Floyd, J. L.; Harper, P. S.; Shaw, D. J. Localisation of the Myotonic Dystrophy Locus to 19q13.2-19q13.3 and Its Relationship to Twelve Polymorphic Loci on 19q. *Hum. Genet.* **1991**, *87*, 73–80.
- (3) Turner, C.; Hilton-Jones, D. The Myotonic Dystrophies: Diagnosis and Management. *J. Neurol., Neurosurg. Psychiatry* **2010**, *81*, 358–367.
- (4) Liquori, C. L.; Ricker, K.; Moseley, M. L.; Jacobsen, J. F.; Kress, W.; Naylor, S. L.; Day, J. W.; Ranum, L. P. Myotonic Dystrophy Type 2 Caused by a CCTG Expansion in Intron 1 of ZNF9. *Science* **2001**, *293*, 864–867.
- (5) Schoser, B.; Timchenko, L. Myotonic Dystrophies 1 and 2: Complex Diseases with Complex Mechanisms. *Curr. Genomics* **2010**, *11*, 77–90.
- (6) Ho, T. H.; Bundman, D.; Armstrong, D. L.; Cooper, T. A. Transgenic Mice Expressing CUG-BP1 Reproduce Splicing Misregulation Observed in Myotonic Dystrophy. *Hum. Mol. Genet.* **2005**, *14*, 1539–1547.
- (7) Mankodi, A.; Takahashi, M. P.; Jiang, H.; Beck, C. L.; Bowers, W. J.; Moxley, R. T.; Cannon, S. C.; Thornton, C. A. Expanded CUG Repeats Trigger Aberrant Splicing of CLC-1 Chloride Channel Pre-mRNA and Hyperexcitability of Skeletal Muscle in Myotonic Dystrophy. *Mol. Cell* **2002**, *10*, 35–44.
- (8) Savkur, R. S.; Philips, A. V.; Cooper, T. A.; Dalton, J. C.; Moseley, M. L.; Ranum, L. P. W.; Day, J. W. Insulin Receptor Splicing Alteration in Myotonic Dystrophy Type 2. *Am. J. Hum. Genet.* **2004**, *74*, 1309–1313.

- (9) Kuyumcu-Martinez, N. M.; Wang, G.-S.; Cooper, T. A. Increased Steady-State Levels of CUGBP1 in Myotonic Dystrophy 1 Are Due to PKC-Mediated Hyperphosphorylation. *Mol. Cell* **2007**, *28*, 68–78.
- (10) Coonrod, L. A.; Nakamori, M.; Wang, W.; Carrell, S.; Hilton, C. L.; Bodner, M. J.; Siboni, R. B.; Docter, A. G.; Haley, M. M.; Thornton, C. A.; Berglund, J. A. Reducing Levels of Toxic RNA with Small Molecules. *ACS Chem. Biol.* **2013**, *8*, 2528–2537.
- (11) Jasinska, A. Structures of Trinucleotide Repeats in Human Transcripts and Their Functional Implications. *Nucleic Acids Res.* **2003**, *31*, 5463–5468.
- (12) Wheeler, T. M.; Leger, A. J.; Pandey, S. K.; MacLeod, A. R.; Nakamori, M.; Cheng, S. H.; Wentworth, B. M.; Bennett, C. F.; Thornton, C. A. Targeting Nuclear RNA for in Vivo Correction of Myotonic Dystrophy. *Nature* **2012**, *488*, 111.
- (13) Konieczny, P.; Selma-Soriano, E.; Rapisarda, A. S.; Fernandez-Costa, J. M.; Perez-Alonso, M.; Artero, R. Myotonic Dystrophy: Candidate Small Molecule Therapeutics. *Drug Discovery Today* **2017**, *22*, 1740–1748.
- (14) Zhang, F.; Bodycombe, N. E.; Haskell, K. M.; Sun, Y. L.; Wang, E. T.; Morris, C. A.; Jones, L. H.; Wood, L. D.; Pletcher, M. T. A Flow Cytometry-Based Screen Identifies MBNL1 Modulators That Rescue Splicing Defects in Myotonic Dystrophy Type I. *Hum. Mol. Genet.* **2017**, *26*, 3056–3068.
- (15) Chamberlain, C. M.; Ranum, L. P. W. Mouse Model of Muscleblind-like 1 Overexpression: Skeletal Muscle Effects and Therapeutic Promise. *Hum. Mol. Genet.* **2012**, *21*, 4645–4654.
- (16) van Agtmaal, E. L.; André, L. M.; Willemsse, M.; Cumming, S. A.; van Kessel, I. D. G.; van den Broek, W. J. A. A.; Gourdon, G.; Furling, D.; Mouly, V.; Monckton, D. G.; Wansink, D. G.; Wieringa, B. CRISPR/Cas9-Induced (CTG.CAG)<sub>n</sub> Repeat Instability in the Myotonic Dystrophy Type 1 Locus: Implications for Therapeutic Genome Editing. *Mol. Ther.* **2017**, *25*, 24–43.
- (17) Lo Scudato, M.; Poulard, K.; Sourd, C.; Tomé, S.; Klein, A. F.; Corre, G.; Huguet, A.; Furling, D.; Gourdon, G.; Buj-Bello, A. Genome Editing of Expanded CTG Repeats within the Human DMPK Gene Reduces Nuclear RNA Foci in the Muscle of DMI Mice. *Mol. Ther.* **2019**, *27*, 1372.
- (18) Sobczak, K.; Wheeler, T. M.; Wang, W.; Thornton, C. A. RNA Interference Targeting CUG Repeats in a Mouse Model of Myotonic Dystrophy. *Mol. Ther.* **2013**, *21*, 380–387.
- (19) González-Barriga, A.; Mulders, S. A.; Van De Giessen, J.; Hooijer, J. D.; Bijl, S.; Van Kessel, I. D.; Van Beers, J.; Van Deutekom, J. C.; Fransen, J. A.; Wieringa, B.; Wansink, D. G. Design and Analysis of Effects of Triplet Repeat Oligonucleotides in Cell Models for Myotonic Dystrophy. *Mol. Ther.–Nucleic Acids* **2013**, *2*, No. e81.
- (20) Childs-Disney, J. L.; Hoskins, J.; Rzuczek, S. G.; Thornton, C. A.; Disney, M. D. Rationally Designed Small Molecules Targeting the RNA That Causes Myotonic Dystrophy Type 1 Are Potently Bioactive. *ACS Chem. Biol.* **2012**, *7*, 856–862.
- (21) Pushechnikov, A.; Lee, M. M.; Childs-Disney, J. L.; Sobczak, K.; French, J. M.; Thornton, C. A.; Disney, M. D. Rational Design of Ligands Targeting Triplet Repeating Transcripts That Cause RNA Dominant Disease: Application to Myotonic Muscular Dystrophy Type 1 and Spinocerebellar Ataxia Type 3. *J. Am. Chem. Soc.* **2009**, *131*, 9767–9779.
- (22) López-Morató, M.; Brook, J. D.; Wojciechowska, M. Small Molecules Which Improve Pathogenesis of Myotonic Dystrophy Type 1. *Front. Neurol.* **2018**, *9*, 349.
- (23) Warf, M. B.; Nakamori, M.; Matthys, C. M.; Thornton, C. A.; Berglund, J. A. Pentamidine Reverses the Splicing Defects Associated with Myotonic Dystrophy. *Proc. Natl. Acad. Sci. U.S.A.* **2009**, *106*, 18551–18556.
- (24) Neaga, I. O.; Hambye, S.; Bodoki, E.; Palmieri, C.; Anseau, E.; Belayew, A.; Oprean, R.; Blankert, B. Affinity Capillary Electrophoresis for Identification of Active Drug Candidates in Myotonic Dystrophy Type 1. *Anal. Bioanal. Chem.* **2018**, *410*, 4495–4507.
- (25) Duncan, R. The Dawning Era of Polymer Therapeutics. *Nat. Rev. Drug Discovery* **2003**, *2*, 347–360.
- (26) Mindemark, J.; Bowden, T. Efficient DNA Binding and Condensation Using Low Molecular Weight, Low Charge Density Cationic Polymer Amphiphiles. *Macromol. Rapid Commun.* **2010**, *31*, 1378–1382.
- (27) Ong, Z. Y.; Fukushima, K.; Coady, D. J.; Yang, Y.-Y.; Ee, P. L. R.; Hedrick, J. L. Rational Design of Biodegradable Cationic Polycarbonates for Gene Delivery. *J. Controlled Release* **2011**, *152*, 120–126.
- (28) Wang, C.-F.; Lin, Y.-X.; Jiang, T.; He, F.; Zhuo, R.-X. Polyethylenimine-Grafted Polycarbonates as Biodegradable Polycarbonates for Gene Delivery. *Biomaterials* **2009**, *30*, 4824–4832.
- (29) Jaworska, J.; Kawalec, M.; Pastusiak, M.; Reczynska, K.; Janeczek, H.; Lewicka, K.; Pamula, E.; Dobrzynski, P. Biodegradable Polycarbonates Containing Side Carboxyl Groups—Synthesis, Properties, and Degradation Behavior. *J. Polym. Sci., Part A: Polym. Chem.* **2017**, *55*, 2756–2769.
- (30) Xu, J.; Liu, Z.-L.; Zhuo, R.-X. Synthesis and in Vitro Degradation of Novel Copolymers of Cyclic Carbonate and D,L-Lactide. *J. Appl. Polym. Sci.* **2006**, *101*, 1988–1994.
- (31) Zhang, Z.; Kuijter, R.; Bulstra, S. K.; Grijpma, D. W.; Feijen, J. The in Vivo and in Vitro Degradation Behavior of Poly(Trimethylene Carbonate). *Biomaterials* **2006**, *27*, 1741–1748.
- (32) Xu, J.; Feng, E.; Song, J. Renaissance of Aliphatic Polycarbonates: New Techniques and Biomedical Applications. *J. Appl. Polym. Sci.* **2014**, *131*, 39822.
- (33) Aied, A.; Greiser, U.; Pandit, A.; Wang, W. Polymer Gene Delivery: Overcoming the Obstacles. *Drug Discovery Today* **2013**, *18*, 1090–1098.
- (34) Blanco, E.; Shen, H.; Ferrari, M. Principles of Nanoparticle Design for Overcoming Biological Barriers to Drug Delivery. *Nat. Biotechnol.* **2015**, *33*, 941–951.
- (35) Suriano, F.; Coulembier, O.; Hedrick, J. L.; Dubois, P. Functionalized Cyclic Carbonates: From Synthesis and Metal-Free Catalyzed Ring-Opening Polymerization to Applications. *Polym. Chem.* **2011**, *2*, 528–533.
- (36) Mespouille, L.; Coulembier, O.; Kawalec, M.; Dove, A. P.; Dubois, P. Implementation of Metal-Free Ring-Opening Polymerization in the Preparation of Aliphatic Polycarbonate Materials. *Prog. Polym. Sci.* **2014**, *39*, 1144–1164.
- (37) Valko, M.; Morris, H.; Cronin, M. Metals, Toxicity and Oxidative Stress. *Curr. Med. Chem.* **2005**, *12*, 1161–1208.
- (38) Nachtergaele, A.; Coulembier, O.; Dubois, P.; Helvenstein, M.; Duez, P.; Blankert, B.; Mespouille, L. Organocatalysis Paradigm Revisited: Are Metal-Free Catalysts Really Harmless? *Biomacromolecules* **2015**, *16*, 507–514.
- (39) Pratt, R. C.; Nederberg, F.; Waymouth, R. M.; Hedrick, J. L. Tagging Alcohols with Cyclic Carbonate: A Versatile Equivalent of (Meth)Acrylate for Ring-Opening Polymerization. *Chem. Commun.* **2008**, 114–116.
- (40) Geihe, E. I.; Cooley, C. B.; Simon, J. R.; Kiesewetter, M. K.; Edward, J. a.; Hickerson, R. P.; Kaspar, R. L.; Hedrick, J. L.; Waymouth, R. M.; Wender, P. a. Designed Guanidinium-Rich Amphipathic Oligocarbonate Molecular Transporters Complex, Deliver and Release siRNA in Cells. *Proc. Natl. Acad. Sci. U.S.A.* **2012**, *109*, 13171–13176.
- (41) Bartolini, C.; Mespouille, L.; Verbruggen, I.; Willem, R.; Dubois, P. Guanidine-Based Polycarbonate Hydrogels: From Metal-Free Ring-Opening Polymerization to Reversible Self-Assembling Properties. *Soft Matter* **2011**, *7*, 9628–9637.
- (42) Cooley, C. B.; Trantow, B. M.; Nederberg, F.; Kiesewetter, M. K.; Hedrick, J. L.; Waymouth, R. M.; Wender, P. a. Oligocarbonate Molecular Transporters: Oligomerization-Based Syntheses and Cell-Penetrating Studies. *J. Am. Chem. Soc.* **2009**, *131*, 16401–16403.
- (43) Zhang, L.-W.; Wang, K.; Zhang, X.-X. Study of the Interactions between Fluoroquinolones and Human Serum Albumin by Affinity Capillary Electrophoresis and Fluorescence Method. *Anal. Chim. Acta* **2007**, *603*, 101–110.
- (44) Michalcová, L.; Glatz, Z. Study on the Interactions of Sulfonyleurea Antidiabetic Drugs with Normal and Glycated Human

Serum Albumin by Capillary Electrophoresis-Frontal Analysis. *J. Sep. Sci.* **2016**, *39*, 3631–3637.

(45) Gonciarz, A.; Kus, K.; Szafarz, M.; Walczak, M.; Zakrzewska, A.; Szymura-Oleksiak, J. Capillary Electrophoresis/Frontal Analysis versus Equilibrium Dialysis in Dexamethasone Sodium Phosphate-Serum Albumin Binding Studies. *Electrophoresis* **2012**, *33*, 3323–3330.

(46) Neaga, I. O.; Bodoki, E.; Hambye, S.; Blankert, B.; Oprean, R. Study of Nucleic Acid-Ligand Interactions by Capillary Electrophoretic Techniques: A Review. *Talanta* **2016**, *148*, 247.

(47) Michalcová, L.; Glatz, Z. Comparison of Various Capillary Electrophoretic Approaches for the Study of Drug-Protein Interaction with Emphasis on Minimal Consumption of Protein Sample and Possibility of Automation. *J. Sep. Sci.* **2015**, *38*, 325–331.

(48) Cho, C. A. H.; Liang, C.; Perera, J.; Liu, J.; Varnava, K. G.; Sarojini, V.; Cooney, R. P.; McGillivray, D. J.; Brimble, M. A.; Swift, S.; Jin, J. Molecular Weight and Charge Density Effects of Guanidinylated Biodegradable Polycarbonates on Antimicrobial Activity and Selectivity. *Biomacromolecules* **2018**, *19*, 1389.

(49) Frère, A.; Kawalec, M.; Tempelaar, S.; Peixoto, P.; Hendrick, E.; Peulen, O.; Evrard, B.; Dubois, P.; Mespouille, L.; Mottet, D.; Piel, G. Impact of the Structure of Biocompatible Aliphatic Polycarbonates on siRNA Transfection Ability. *Biomacromolecules* **2015**, *16*, 769–779.

(50) Frère, A.; Baroni, A.; Hendrick, E.; Delvigne, A.-S.; Orange, F.; Peulen, O.; Dakwar, G. R.; Diricq, J.; Dubois, P.; Evrard, B.; Remaut, K.; Braeckmans, K.; De Smedt, S. C.; Laloy, J.; Dogné, J.-M.; Feller, G.; Mespouille, L.; Mottet, D.; Piel, G. PEGylated and Functionalized Aliphatic Polycarbonate Polyplex Nanoparticles for Intravenous Administration of HDAC5 siRNA in Cancer Therapy. *ACS Appl. Mater. Interfaces* **2017**, *9*, 2181–2195.

(51) Kustermann, S.; Boess, F.; Bunes, A.; Schmitz, M.; Watzele, M.; Weiser, T.; Singer, T.; Suter, L.; Roth, A. A Label-Free, Impedance-Based Real Time Assay to Identify Drug-Induced Toxicities and Differentiate Cytostatic from Cytotoxic Effects. *Toxicol. In Vitro* **2013**, *27*, 1589–1595.

(52) Rundlett, K. L.; Armstrong, D. W. Methods for the Estimation of Binding Constants by Capillary Electrophoresis. *Electrophoresis* **1997**, *18*, 2194–2202.

(53) Colton, I. J.; Carbeck, J. D.; Rao, J.; Whitesides, G. M. Affinity Capillary Electrophoresis: A Physical-Organic Tool for Studying Interactions in Biomolecular Recognition. *Electrophoresis* **1998**, *19*, 367–382.

(54) Chen, Z.; Weber, S. G. Determination of Binding Constants by Affinity Capillary Electrophoresis, Electrospray Ionization Mass Spectrometry and Phase-Distribution Methods. *Trends Anal. Chem.* **2008**, *27*, 738–748.

(55) Vamecq, J.; Maurois, P.; Pages, N.; Bac, P.; Stables, J. P.; Gressens, P.; Stanicki, D.; Vanden Eynde, J. J. 1,2-Ethane Bis-1-Amino-4-Benzamidine Is Active against Several Brain Insult and Seizure Challenges through Anti-NMDA Mechanisms Targeting the 3H-TCP Binding Site and Antioxidant Action. *Eur. J. Med. Chem.* **2010**, *45*, 3101–3110.

(56) Tran, N. T.; Taverna, M.; Miccoli, L.; Angulo, J. F. Poly(Ethylene Oxide) Facilitates the Characterization of an Affinity between Strongly Basic Proteins with DNA by Affinity Capillary Electrophoresis. *Electrophoresis* **2005**, *26*, 3105–3112.

(57) Busch, M. H. A.; Carels, L. B.; Boelens, H. F. M.; Kraak, J. C.; Poppe, H. Comparison of Five Methods for the Study of Drug-Protein Binding in Affinity Capillary Electrophoresis. *J. Chromatogr. A* **1997**, *777*, 311–328.

(58) xCELLigence RTCA DP Real Time Cell Analyzer—Dual Purpose.